Novel interactions within the SIR heterochromatin complex potentiate inter-subunit communication and gene repression

Jenna Kotz[1,2,3], E. J. Martz[1,2,3], Maya Nelson[1], Nicole Savoie[1], Lauren Schmitt[1,2], Jordan States[1], Nathan Holton[1], Kirk Hansen[1,2], and Aaron M. Johnson[1,2]

[1]Department of Biochemistry and Molecular Genetics

[2]Structural Biology, Biochemistry, and Biophysics Program

University of Colorado, Denver – Anschutz Medical Campus

[3]These authors contributed equally

To whom correspondence should be addressed: Aaron M. Johnson, Dept. of Biochemistry and Molecular Genetics, University of Colorado School of Medicine, 12801 E. 17th Ave., Aurora, CO 80045. Tel.: 303-724-3224; Fax: 303-724-3215; E-mail: aaron.m.johnson@CUAnschutz.edu

Keywords: epigenetics, yeast, sirtuin, heterochromatin, HDAC, crosslinking-mass spectrometry

ABSTRACT

Organisms with smaller genomes often perform multiple functions using one multi-subunit protein complex. The *S. cerevisiae* Silent Information Regulator complex (SIRc) carries out all of the core functions of heterochromatin. SIR complexes first drive the initiation and spreading of histone deacetylation in an iterative manner. Subsequently, the same complexes are incorporated stably with nucleosomes, driving compaction and repression of the underlying chromatin domain. These two distinct functions of SIRc have each been characterized in much detail, but the mechanism by which the dynamic spreading state switches to stable compaction is not well-understood. This incomplete knowledge of potential intra-complex communication is partly due to a lack of structural information of the complex as a whole; only structures of fragments have been determined to date. Using cross-linking mass spectrometry in solution, we identified a novel inter-subunit interaction that physically connects the two states of SIRc. The Sir2 deacetylase makes direct interactions with the scaffolding subunit Sir4 through its coiled-coil domain, which also interacts with the Sir3 compaction/repression subunit. Within the hub of interactions are conserved residues in Sir2 that can sense deacetylation state, as well as amino acids that likely diverged and co-evolved to interact with Sir4, promoting species-specific functions. Mutation of this interaction hub disrupts heterochromatic repression, potentially by disrupting a conserved mechanism that communicates completion of deacetylation to switch to compaction. Our work highlights how a single multi-functional chromatin regulatory complex can stage a step-wise mechanism that requires a major transition in activities to achieve epigenetic gene repression.

45 **INTRODUCTION**

46 Budding yeast heterochromatin is a powerful simplified model to study chromatin-mediated gene
47 silencing[1, 2]. The SIR complex is a stripped-down heterochromatin machine, necessary and sufficient
48 for transcriptional repression. Yeast heterochromatin shares a basic mechanism of formation with
49 heterochromatin in all eukaryotes separated by a dynamic phase: recruitment of a histone modifying
50 complex to a region targeted for silencing, nucleation of heterochromatin by histone modification and
51 sequence-independent spreading of silencing across larger regions of the genome, dependent on
52 binding of a heterochromatin protein to the modified histone; and a stable phase characterized by
53 compaction of the genome (Figure 1A). The SIR complex incorporates Sir2, an NAD^+-dependent histone
54 deacetylase (HDAC), conserved in all eukaryotes, whose activity is required for silencing[3, 4]. The SIR
55 complex (Fig. 1B,C) is scaffolded by the Sir4 subunit, and Sir3 reads the histone modification pattern and
56 allows the SIR complex to compact nucleosomes only when they have certain modifications erased,
57 including de-acetylation of histone H4 lysine 16 (H4K16), which is critical for gene silencing. SIR
58 heterochromatin stably and heritably silences the genes that dictate mating-type cell differentiation and
59 genes in subtelomeric regions. A wealth of genetic and biochemical data from the SIR system has
60 developed one of the richest models of heterochromatin regulation that is ripe for a new level of
61 mechanistic structure-function analysis. The in vitro SIR heterochromatin biochemical system that we
62 have developed in budding yeast[5] has established a model to study a stripped-down silencing
63 mechanism with unprecedented detail.

64 A subset of molecular interactions that are important for SIR complex mechanism have been captured
65 through high-resolution crystal structures; however, the nature by which these interactions cooperate
66 within the full SIR complex to carry out its functions is not clear. The Sir3 BAH domain binds directly to
67 the nucleosome via the histone H4 tail and multiple histones in the globular core of the nucleosome,
68 captured by crystal structures[6-9]. The BAH domain is less than 25% of Sir3 and a small fraction of the
69 full SIR complex, yet structures of the BAH-nucleosome offer the only major structural insights into SIR-
70 nucleosome interactions. Structures of other domains of Sir3 and Sir2 and small fragments of Sir4 have
71 also been solved[10-14]. Though these structures give less insight into the interactions with the

72 nucleosome, they do provide reference points for biophysical approaches that can identify intermolecular
73 interactions, such as cross-linking mass spectrometry[15].

74 Removal of histone modifications that promote transcription and open chromatin is essential for
75 heterochromatin establishment in all organisms. In budding yeast, the heterochromatin histone code is
76 the absence of nearly all modifications, while many organisms erase the same modifications as the SIR
77 complex and add others, such as H3 lysine 9 and 27 methylation[16]. Sir2 is an NAD^+-dependent lysine
78 de-acetylase, which can remove many acetyl modifications to histone lysines[5, 17]. The SIR complex
79 can bind directly to acetylated chromatin, engaging via Sir4-nucleosome interactions that are poorly-
80 understood[5, 18]. Sir3 is bridged by Sir4 in this conformation, poised for action. Sir2 acts first,
81 preferentially de-acetylating histone H4K16, which Sir3 then binds tightly to in the de-acetylated state.
82 De-acetylation of additional histone lysines in the tails and core of the nucleosome by Sir2 facilitates
83 chromatin compaction and reduces chromatin remodeling. Step-wise conformational changes during de-
84 acetylation have been suggested by us and others[5, 19, 20], based on the two-step model for Sir3
85 interactions as it locks down onto the nucleosome after H4K16 de-acetylation. These changes may affect
86 the orientation of Sir2 as it proceeds through erasure of all acetylation to facilitate Sir3-mediated
87 compaction. At present, our models for these states of the SIR complex are coarse-grained and require
88 improved methods for capturing these conformational switches.

89 We characterized the SIR heterotrimer by cross-linking mass spectrometry in solution. By doing so,
90 we identified a novel protein-protein interface between Sir2 and the coiled-coil domain of Sir4. The coiled
91 coil was previously demonstrated to associate with Sir3, suggesting this may be a hub of communication,
92 connecting the early steps of the SIRc mechanism to the later. A key tyrosine in this interaction region of
93 Sir2, conserved in nearly all eukaryotic sirtuins, is positioned to sense deacetylation state. In contrast, a
94 pair of amino acids adjacent to the tyrosine may have co-evolved to interact specifically with Sir4 as a
95 means of inter-subunit communication. By CRISPR genome editing, we mutated these two features of
96 Sir2 and demonstrated that they each are critical for proper heterochromatin gene silencing. Our work
97 highlights how a single multi-functional chromatin regulatory complex can stage a step-wise mechanism
98 that requires a major transition in activities to achieve epigenetic gene repression.

99

100 **RESULTS**

101 **Cross-linking mass spectrometry of the SIR complex reveals novel interactions**

102 Because there is a lack of atomic-resolution structural information for the heterotrimeric SIR complex, we
103 used cross-linking mass spectrometry to gain insight into specific protein-protein interactions, mapping
104 inter-subunit cross-links between specific amino acids (Figure 2A). Purified SIR subunits with specific
105 truncations to promote solubility and decrease higher-order interactions were used. Subunits were pre-
106 incubated to form the complex and then subjected to cross-linking using the zero-length cross-linker
107 DMTMM which cross-links lysines directly to aspartic and glutamic acid residues. Proteins were
108 trypsinized and separated by strong cation exchange (SCX) chromatography to enrich for crosslinked
109 peptides in specific fractions (Figure 2B) that were then subjected to tandem mass spectrometry (MS/MS).
110 Cross-links were identified using pLink analysis software[21, 22].

111 Mapping of peptide cross-links demonstrated many well-defined self cross-links within each protein,
112 including identical peptide homo-meric cross-links of two identical peptides in the Sir4 coiled-coil (Sir4-
113 CC), as expected for that dimerization region (Supplemental Figure S1). We focused our attention on the
114 inter-protein cross-links to gain insight into the conformation of the SIR complex (Figure 2C). While the
115 inter-subunit cross-links were more sparse than for intra-subunit, this is in keeping with the limited
116 previously-identified interaction surfaces. We validated the known interactions between the Sir4 coiled-
117 coil and the middle of Sir3(amino acids 485-515)[12] and also the interaction of Sir2 and the Sir2
118 Interaction Domain (SID) of Sir4 that promotes the Sir2/4 sub-complex[10] (Figure 2D). Unexpectedly,
119 we also identified multiple peptide cross-links between Sir2 and the coiled-coil of Sir4 (Figure 2E), which
120 have not been previously identified by genetic or biophysical approaches. The proximity of the novel Sir2
121 interaction on the Sir4 coiled-coil to the known Sir3 binding site suggests a potential hub of interactions
122 within the SIR complex. This is supported by other novel cross-links between Sir2 and Sir3(Figure 2F),
123 surprising because these two proteins have never been suggested to physically interact.

124

125 **Sir2 directly interacts with the coiled-coil domain of Sir4**

126 We next determined whether the interaction we observed via crosslinking of Sir2 to the Sir4-CC was
127 dependent on the known inter-subunit interactions within the SIR complex using two additional
128 crosslinking mass spectrometry experiments. The proximity of residues on the Sir4-CC that crosslink to
129 Sir2 and residues on the Sir4-CC that disrupts Sir3 interaction when mutated (Figure 3A), suggests either
130 that Sir3 orients the Sir4-CC to interact with Sir2 or that the Sir4-CC is a potential hub of communication
131 between activities of Sir2 and Sir3. We wished to test the first of these possibilities, whether the
132 interaction with Sir3 may orient the Sir4 coiled-coil for interaction with Sir2, by omitting Sir3 in incubation
133 of Sir4ΔN and Sir2 (Figure 3B,C). Second, we tested if the extensive interaction between the Sir4 SID
134 and Sir2 was required for Sir2 to make additional contacts at the distal coiled-coil on Sir4, or whether the
135 coiled-coil of Sir4 could bind Sir2 independently (Figure 3D). In both cases, we consistently observed
136 cross-links between Sir2 and the coiled coil of Sir4, demonstrating a novel, independent interaction
137 across this interface within the SIR complex.

138 To characterize the interaction between Sir2 and the Sir4-CC further, we performed microscale
139 thermophoresis (MST) experiments titrating the Sir4-CC into a solution of fluorescently-labeled, his-
140 tagged Sir2 (Figure 3E). Binding between the two was observed, though the affinity was relatively low,
141 compared to that of the Sir4-SID binding to Sir2 (Figure 3F). The lower affinity interaction of the Sir4-CC
142 with Sir2 suggests that this interaction may not be a primary driver of association of the two full-length
143 proteins, but instead may occur intermittently, perhaps in a regulated manner.

144

145 **Identification of Sir2 279-286 as a novel region that is important for silencing *in vivo***

146 We next aimed to determine whether the interaction between Sir2 and the Sir4-CC may be
147 important for the regulation of gene silencing in *S. cerevisiae*. We used a previously-designed yeast strain
148 bearing GFP and RFP reporter genes at the *HMR* and *HML* loci, respectively[23, 24] (Figure 4A). When
149 the SIR complex activity is disrupted, both reporters are de-repressed and the colonies and cells
150 fluoresce. CRISPR genome editing was used to make markerless edits to the *SIR* genes to mutate
151 residues within major cross-linking regions, assessed by high frequency of cross-links and thresholding.

152 Two regions of Sir2 were the primary focuses of the mutational analysis, residues 131-135 and
153 279-286 (Figure 4B), neither of which had been previously identified as interacting with another protein
154 and no mutations with phenotypes had been previously reported for either region. We first created mutant
155 strains in which all amino acids in either region were mutated to alanines. The mutation of amino acids
156 279-286 led to de-repression of the HM loci by colony fluorescence, comparable to a mutation of Sir2
157 that abolishes the deacetylation activity, H364Y [25] (Figure 4C). We also confirmed that this de-
158 repression was not caused by overall destabilization and degradation of the protein (Figure 4D).
159 Conversely, mutating 131-135, nor in other crosslinking sites, did not lead to significant de-repression
160 and fluorescence (Figure 4C, Supplemental Figure S2).

161

162 **Sir4-CC interacts with a conserved sensor region of Sir2**

163 The Sir2 residues that interact with the Sir4-CC are adjacent to the highly-conserved cofactor
164 binding loop (CBL) of Sir2, widely found in sirtuins [26, 27] (Figure 5A,B). The CBL adopts many
165 conformations in the available sirtuin crystal structures, typically depending on the state of cofactor
166 binding. NAD+-bound sirtuin structures tend to have a closely-packed, ordered CBL that makes explicit
167 contact with the cofactor bound, while crystal structures without cofactor bound typically have less
168 ordered or flexible and unresolved CBLs (Figure 5C). The adjacent region to the CBL, the stretch of
169 amino acids that includes the specific Sir4-CC cross-link site at Sir2-K283, which we henceforth term the
170 cofactor binding loop extension, is itself highly-conserved in a subset of sirtuins, from yeast to humans
171 (Figure 5A). For example, human sirtuins SIRT1, 2, 3, 4, and 5 all have a conserved tyrosine,
172 corresponding to Y281 in *S. cerevisiae*, yet SIRT6 and SIRT7 do not. This tyrosine is conserved in *S.*
173 *cerevisiae* sirtuins Hst1,2, and 3, but not Hst4. The CBL extension has conserved residues that, in some
174 sirtuin crystal structures, point towards and/or make hydrogen bonding interactions with the ribose or
175 nicotinamide moiety of NAD+. Y281 (in ScSir2) in particular has been observed to do this, for example
176 in the Sir2/Sir4-SID crystal structure with ADP-ribose bound [10], and a structure of ScSir2 in the act of
177 deacetylation also has Y281 pointing toward the deacetylation intermediate. The conservation of certain
178 residues within the CBL extension and the physical interaction that it makes with Sir4CC is highly

179 suggestive of a means to couple the sensing of NAD+, by residues such as Y281, with communication
180 to the Sir4CC, and possibly to its other binding partner Sir3.
181
182 **Mutational dissection reveals two essential components for silencing in the Sir2 279-286 region**
183 To determine which residues are important for silencing within the 279-286 region, we began by
184 mutating each tandem two amino acid pair and assessing colony fluorescence. We observed specific
185 pairs with increased fluorescence, centering on Sir2 residues G279, F280, Y281, as well as K283 and
186 I284 (Figure 5D).
187 While the colony-based fluorescence was useful for screening purposes, we next turned to a
188 more quantitative readout, using single-cell imaging. This approach allows us to not only provide a more
189 accurate fluorescence intensity quantification but also profiles many cells in the same genetic background,
190 to determine if there is more than one distinct population. For example, variegation in the population can
191 lead to a bimodal distribution of cells, some of which have repressed GFP while other cells have de-
192 repressed HM loci and subsequently the fluorescent reporters. Using this single-cell method, we were
193 able to quantitatively distinguish strains that repressed the HM loci versus those where SIR-based
194 repression was disrupted. We first characterized the mutant in the 279-286 patch, which exhibited de-
195 repression of the HM loci, as expected, by visual inspection of single cells by fluorescence microscopy
196 (Figure 6A). Quantification demonstrated that Sir2 279-286A cells have fluorescent signal similar to the
197 catalytic mutant Sir2 H364Y, slightly lower than a full deletion of Sir2. Single-cell quantitative profiling of
198 the double mutants in the Sir2 279-286 patch demonstrated that Sir2 280-281A and 281-282A mutants
199 were de-repressed at HM to the same extent as the Sir2 deletion mutant (Figure 6B). Since both of these
200 double-mutants contained the Sir2 Y281A mutation, we profiled this single mutant and found that it
201 displayed the same phenotype as the Sir2 delete. A similar strong phenotype was observed for the Sir2
202 283-284A double-mutant, although other double-mutants containing one, but not the other, of these two
203 mutations did not produce a phenotype, suggesting that these two residues are together important for
204 SIR-dependent repression.

205 As an orthogonal quantitative technique to determine the effect of Sir2 mutations, we use RT-
206 qPCR for the GFP and RFP reporter genes and in addition assayed for expression of two subtelomeric
207 genes that were previously reported to be de-repressed when *SIR* genes were deleted [28]. Compared
208 to WT, the Y281A and 283-284A mutants both displayed a loss of silencing, resulting in >1000-fold
209 upregulation of the GFP and RFP reporter genes in the *HM* loci, comparable to the catalytic mutant of
210 Sir2 (Figure 6D). Interestingly, the subtelomeric genes *CHA1* and *IMD2* were only de-repressed in the
211 Sir2 Y281A mutant.

212

213 **DISCUSSION**

214 We set out to more fully map the protein-protein interactions that occur within the SIR complex
215 and identified a novel interaction interface that is required for SIR heterochromatin, potentially via
216 coordinating a transition from the early steps in the mechanism to the later steps. Using cross-linking
217 mass spectrometry of the SIR complex allowed us to identify these novel interactions between Sir2 amino
218 acids 279-286 and the Sir4 coiled-coil domain, which were further supported by microscale
219 thermophoresis of Sir2 with Sir4 coiled-coil. Subsequently, we mutated these regions by CRISPR editing
220 of the endogenous *SIR* genes to uncover the Sir2 279-286 region as an important regulator of SIR-
221 dependent epigenetic gene repression. These novel connections between Sir2 and the region on Sir4
222 that is already known to bind Sir3 suggest a mode of coordination between the early events of Sir2
223 deacetylation of nucleosomes and the subsequent stable binding of those deacetylated nucleosomes by
224 Sir3 that converts the chromatin to a compact, repressed state. Our work helps uncover how a single
225 multi-functional heterochromatin complex, sufficient to carry out all the core steps of epigenetic gene
226 repression, can coordinate diverse activities.

227

228 *Triangulation of the SIR complex subunits by the Sir4 coiled-coil*

229 Using cross-linking mass spectrometry of the SIR complex allowed us to identify a previously-
230 uncharacterized interaction between Sir2 and the Sir4 coiled-coil. This interaction is not critical to Sir2-
231 Sir4 association, due to the higher-affinity between Sir2 and the central Sir2-interacting domain (SID) of

232 Sir4, which is stable enough to be co-purified and co-crystallized [10]. The nature of this weaker Sir2-
233 Sir4 coiled coil interaction suggests that it may be dynamic, offering the opportunity for conformational
234 change within the SIR complex where Sir2 can bind to the Sir4 coiled-coil transiently, potentially at a
235 specific step in the mechanism of heterochromatin formation. The proximity of the regions of the Sir4
236 coiled-coil that interact with Sir2 and those that interact with Sir3 suggest that a dynamic mode of Sir2
237 binding could be transmitted to Sir3 through the Sir4 coiled-coil. In support of the potential for coordination,
238 we identified an additional novel Sir2-Sir3 interaction (Figure 2F), the first to be discovered between these
239 two subunits. While this singular point of crosslinking between Sir2 and Sir3 may not be evidence of a
240 significant subunit interface that can directly influence the SIR mechanism, it provides further evidence
241 in favor of the Sir4 coiled-coil as a triangulation hub between the subunits, perhaps as a conduit of
242 information between Sir2's dynamic deacetylation mode and Sir3's stable lockdown mode. Finally, it is
243 notable that the Sir2 279-286 region that is critical for gene repression was crosslinked to the Sir4 coiled-
244 coil only in the absence of Sir3, suggesting that there may be some level of influence that can shift the
245 interactions.
246
247 *Coordination of the Sir2 cofactor binding loop extension residues as a potential mode-switching*
248 *mechanism for the SIR complex*
249 To our knowledge, no mutant from S277-L286 has been isolated in a screen or characterized
250 individually for silencing activity or Sir2 activity. Mutants of F274, R275, and S276, the last residues of
251 the CBL, have been characterized as silencing mutants and demonstrate a variety of effects on Sir2
252 activities [29-31] and CBL deletions lead to loss of silencing [32]. R275 is deficient for silencing, but in
253 vitro histone peptide deacetylation is not affected [29]. Fusions that replace the catalytic components of
254 Sir2 with fairly conserved regions from other species frequently fail to complement in gene silencing [32,
255 33]. While the CBL extension has some conserved residues, others, such as the critical K283 and I284
256 combination, are not conserved, suggesting that the coupling to Sir4 is lost by these fusions. Sherman
257 et al. showed that the swap of the human SIRT2 catalytic domain into yeast Sir2 is dominant negative,
258 suggesting that the mutant could bind to Sir4 but not carry out the full mechanism; rDNA silencing was

intact in the fusion [32]. Mead et al. demonstrated that swapping singular regions of Sir2 into Hst1 was not sufficient to restore SIR silencing; however no combinations that included the main Sir4 binding domain and the region around the CBL were constructed. The regulatory mechanism involving the extended cofactor binding loop in Sir2 depends on NAD+, since a catalytic domain that does not depend on NAD+ subverts this regulatory mechanism [34]. These previous findings support the importance of the novel Sir2-Sir4CC interaction that we have identified in driving NAD+-dependent formation of SIR heterochromatin.

With our current study and in light of the previous work outlined above, we propose a model in which Sir2 Y281 senses active site occupancy and this is communicated via residues K283 and I284 that make direct interactions with the Sir4 coiled-coil, preventing the “lockdown” stage of the mechanism (Figure 7). Once deacetylation is complete, the sensor is required to switch to the next mode. This may explain why a Y281A sensor mutant displays a stronger phenotype, de-repressing subtelomeric genes, by preventing the licensing step. The 283-284A mutant may simply bypass the sensor, removing the hold on the “lockdown” stage, allowing from some repression to occur. The wild-type function of this staging could be important for the tight, >1000-fold repression at the *HM* loci, but dispensable for tuning subtelomeric genes. When both elements are mutated in the 279-286A mutant, the 283-284A mutation suppresses the Y281A mutation by allowing the “lockdown” stage to occur, even in the absence of the sensor that stages the mechanism for the strongest repression.

Conclusion

Our work using cross-linking mass spectrometry as a means of probing the SIR heterotrimer led to identification of inter-subunit physical interactions that had not be previously identified, despite a rich history of SIR genetics and biochemistry. The specific Sir2-Sir4 interface we characterize sits poised to sense completion of deacetylation and license the second half of them mechanism where Sir3 locks down on chromatin to repress transcription. This mechanism may be conserved as a means to stage deacetylation that is coupled to secondary coordination within many sirtuin complexes with diverse functions.

286

287

288

289 **METHODS**

290 *Sir Protein Purifications*

291 Recombinant Sir3 was purified as described in [5], via FLAG purification for both full-length and winged
292 helix deletion (Sir3 1-850). Sir2 (untagged final) was expressed in E. coli as a GST fusion and purified
293 by glutathione affinity chromatography and PreScission Protease cleavage. Sir2-6XHis was expressed
294 in E. coli and purified by via Ni-NTA and MonoQ chromatography steps and finally dialyzed into 30 mM
295 Hepes pH 7.5, 100 mM NaCl, 5% glycerol. Sir4 constructs were all cloned downstream of maltose-
296 binding protein (MBP) and expressed in E. coli. MBP fusions were purified via amylose resin
297 chromatography and elution with maltose. Sir4(744-1358, "Sir4-ΔN) and Sir4(744-115, Sir4-SID+) were
298 further purified by MonoS chromatography. All Sir4 preps were dialyzed into 50 mM Hepes pH 7.5, 100
299 mM NaCl, 1 mM DTT, 5-10% glycerol.

300

301 *Crosslinking Mass Spectrometry*

302 Crosslinking was performed at neutral pH, 35°C for 1hr and quenched with Ammonium bicarbonate.
303 Trypsin peptides were separated by strong cation exchange chromatography where the crosslinked
304 peptides with higher total charge generally elute later from the gradient (Fig. 2B). Tandem mass
305 spectrometry (MS/MS) analysis was run and cross-links were identified using a data-dependent
306 acquisition method on a Fusion-Lumos. The method was optimized and biased towards peptides found
307 in higher charge states(z > 2+). Cross-links were further identified using pLink analysis software[21, 22].
308 Analysis of the SIR complex used E. coli-derived Sir2 and a large fragment of Sir4(744-1358) as a
309 maltose binding protein fusion. To minimize oligomerization for XL-MS, to better define unique protein-
310 protein interactions, a Sir3 construct with deleted winged helix dimerization domain was used, purified
311 as described yeast overexpression [5]. This left the Sir4 dimeric coiled-coil region (Sir4cc) at the C-
312 terminus as the single self-interaction domain, which cannot be deleted without disrupting Sir3

313 interactions in the SIR complex[35]. Circular crosslink figures were generated with xiView
314 (https://xiview.org/) with a minimum match score of 27. Experiments in Figure 3 were further thresholded
315 by masking any Sir2 or Sir4 site that was also frequently crosslinked non-specifically to maltose binding
316 protein in the Sir4 fusion constructs (Supplemental Table S1). Experiments in Figure 3 were displayed
317 as a matrix for added resolution. All data are publicly available on the Proxl server;
318 http://www.yeastrc.org/proxl_public/projectReadProcessCode.do?code=hmj2tvem8kxpnrn0vt8o995yx8aeltd
319 6jh4giyl2tyv9sq4pd3iosp01d3ufs8r
320
321 *Microscale thermophoresis (MST)*
322 MST was performed on a NanoTemper Technologies Monolith NT.115 pico instrument, medium power,
323 auto-detect excitation, Pico-RED excitation color with RED-tris-NTA labeling of Sir2-6Xhis, 24-25ºC, for
324 all experiments. All experiments performed with constant Sir2-6Xhis in 30 mM Hepes pH 7.9, 100 mM
325 NaCl. 10 nM Sir2-6Xhis was used for Sir4(744-1358, "Sir4-ΔN) and Sir4(744-115, Sir4-SID+) and 50 nM
326 for Sir4(1150-1358, Sir4-CC+). MO Affinity Analysis software was used for binding curve fitting and Kd
327 value determination.
328
329 *Amylose Bead Pulldown*
330 Untagged Sir2 was incubated with MBP-tagged Sir4 constructs at 16ºC for 1 hr in Binding Buffer (50 mM
331 Hepes pH 7.9, 200 mM NaCl, 10% glycerol, 1 mM DTT, 0.1% Tween-20). 50 µL amylose resin was
332 added and incubated at 16ºC for 1 hr on a Thermomixer at 1000 rpm. Beads were collected at 4ºC by 1
333 min centrifugation at 500 x g, washed with 75 µL Binding Buffer, then protein was eluted in the wash
334 buffer with 10 mM maltose by 5 min. mixing at 23ºC and 1 min centrifugation at 500 x g 4ºC. Samples
335 were mixed with 2X Bio-Rad SDS Sample Buffer and run on a 12% polyacrylamide gel with Coomassie
336 stain.
337
338 *CRISPR genome editing*
339 Plasmid pML104 (Addgene #67638) was used for CRISPR-Cas9 yeast genome editing as previously
340 described [36]. pML104, containing Cas9 and an sgRNA cassette, was digested with SwaI and BclI, then

341 ligated with annealed oligonucleotides to serve as the guide sequence for the sgRNA. Donor DNA was
342 with the target mutation, along with a silent PAM site mutation to prevent re-cutting of the genomic DNA,
343 was produced by PCR from previously-generated plasmid or by gBlock synthesis (IDT). Donor DNAs
344 included ~40-70 bp of homology on either side to promote homologous recombination DNA repair. Where
345 necessary, silent mutations between the Cas9 cut site and the target mutation were made to limit
346 recombination before the target editing site. Yeast strains were transformed with 1 µg of pML104 and 3
347 µg of donor DNA using lithium acetate and PEG. Mutants were confirmed by extracting genomic DNA
348 with lithium acetate and SDS, amplifying the target gene, and sequencing. Cells were counter-selected
349 on 5-fluoroorotic acid (5-FOA) plates to remove the pML104 plasmid. All yeast strains generated listed
350 in Supplemental Table S2.
351
352 *FLAME assays by colony*
353 Yeast colonies were grown from glycerol stock on synthetic complete medium plates for 2-3 days.
354 Colonies were imaged on an AMG EVOS imager in transillumination and GFP channel using 30%
355 fluorescence threshold at 4X magnification.
356
357 *Single cell FLAME assays*
358 Yeast strains were grown in synthetic complete medium with glucose to 0.3-0.5 OD, transferred to 96-
359 well plates and imaged on an EVOS microscope at 40X objective for transmission, GFP, and RFP
360 collection. Images were analyzed by FIJI. First, transmission images were used to make a mask of >100
361 individual cell outlines, along with background outlines. The mask is then used to collect intensity data
362 for GFP and RFP images. Background-subtracted values were visualized in violin plot format with
363 Student's t-test for statistical significance.
364
365 *RT-qPCR*
366 RNA was extracted from yeast using hot acid phenol and SDS, followed by a wash with chloroform and
367 ethanol precipitation. Samples were treated with Turbo DNase and cleaned up with the Qiagen RNeasy

368 Mini Kit. cDNA was produced using the Applied Biosystems High Capacity cDNA Reverse
369 Transcription Kit. qPCR was performed using the SYBR GreenER qPCR SuperMix Universal (Thermo)
370 under standard conditions using the primers in Supplemental Table 3.
371

372

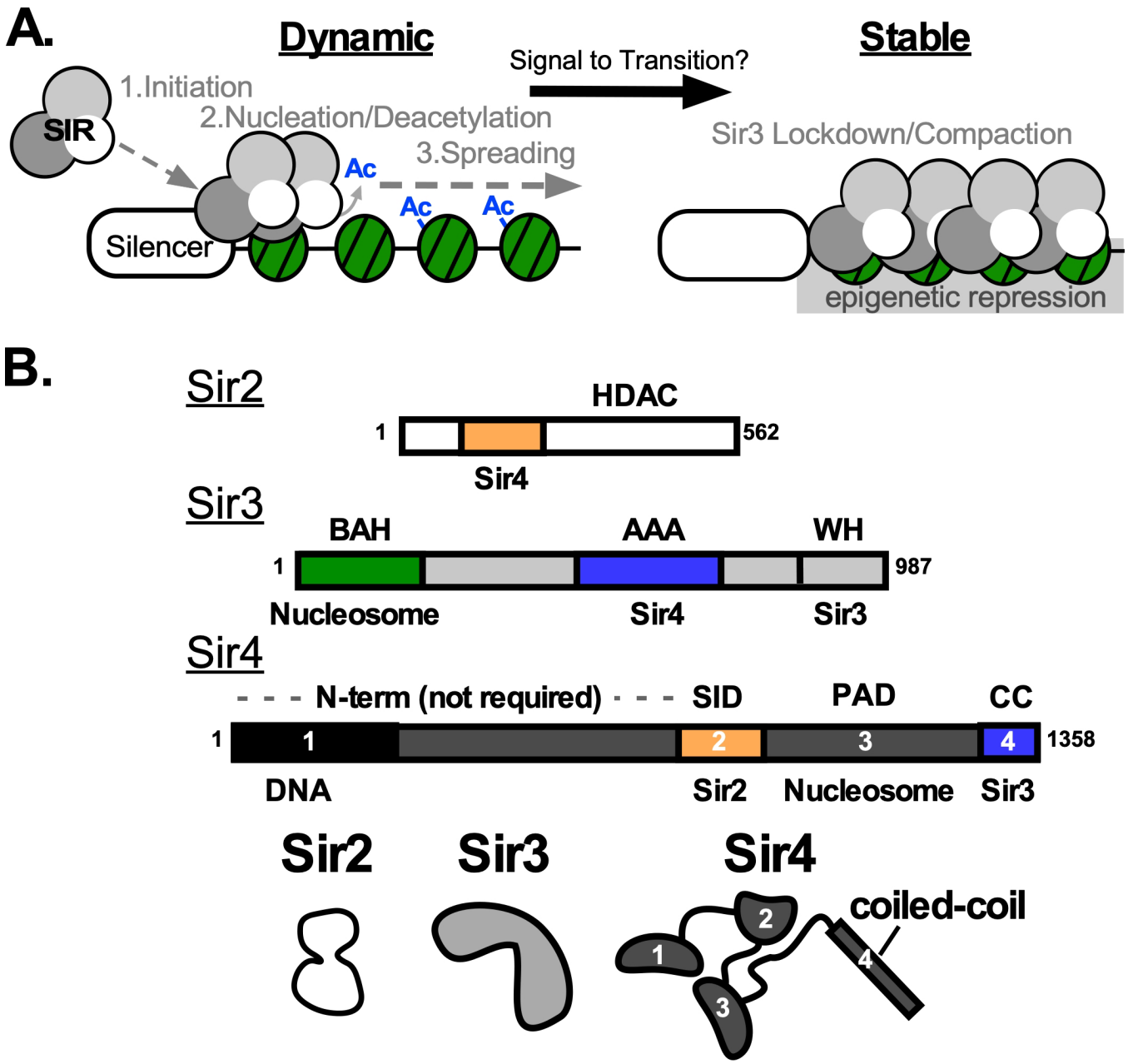

373

374 **Figure 1. Mechanism and architecture of the SIR system.** A) SIR heterochromatin works in two
375 primary modes: 1) a dynamic mode of recruitment of the SIR complex to target sites on chromatin which
376 then leads to nucleation of the histones by deacetylation and spreading of this part of the mechanism to
377 contiguously deacetylate the region, 2) a stable mode where the Sir3 subunit coordinates compaction of
378 chromatin by the SIR complex and stable incorporation of the complex into the heterochromatin domain.
379 After initiation, the mechanism spreads and represses in a sequence-independent epigenetic manner,
380 where the extent of spread of the domain can be inherited. As noted, a major question that remains in

381 the field is how the singular, muti-functional SIR complex switches from one mode to the next, since the
382 Sir2 active site directly competes with the Sir3 lockdown site. B) Domain structure of the core SIR
383 subunits. Sir2, an NAD+-dependent histone deacetylase (HDAC), has a core catalytic HDAC domain
384 downstream of a region that interacts with the Sir4 subunit. Sir3 has an N-terminal bromo-adjacent
385 homology (BAH) domain that binds to a nucleosome that is deacetylated at histone H4 K16. A non-
386 canonical AAA ATPase domain, missing catalytic residues, is in the middle of the protein and this region
387 binds Sir4. At its C-terminus, Sir3 has a winged-helix domain that can dimerize the protein. Sir4 has an
388 N-terminal region of ~750 amino acids that has DNA binding activity, but is not absolutely required for
389 SIR function. Next downstream is the Sir2-Interaction Domain (SID), then a Partitioning and Anchoring
390 domain (PAD) that makes contacts with nuclear periphery proteins, and the C-terminal coiled coil domain
391 that dimerizes and makes interactions with Sir3.
392
393

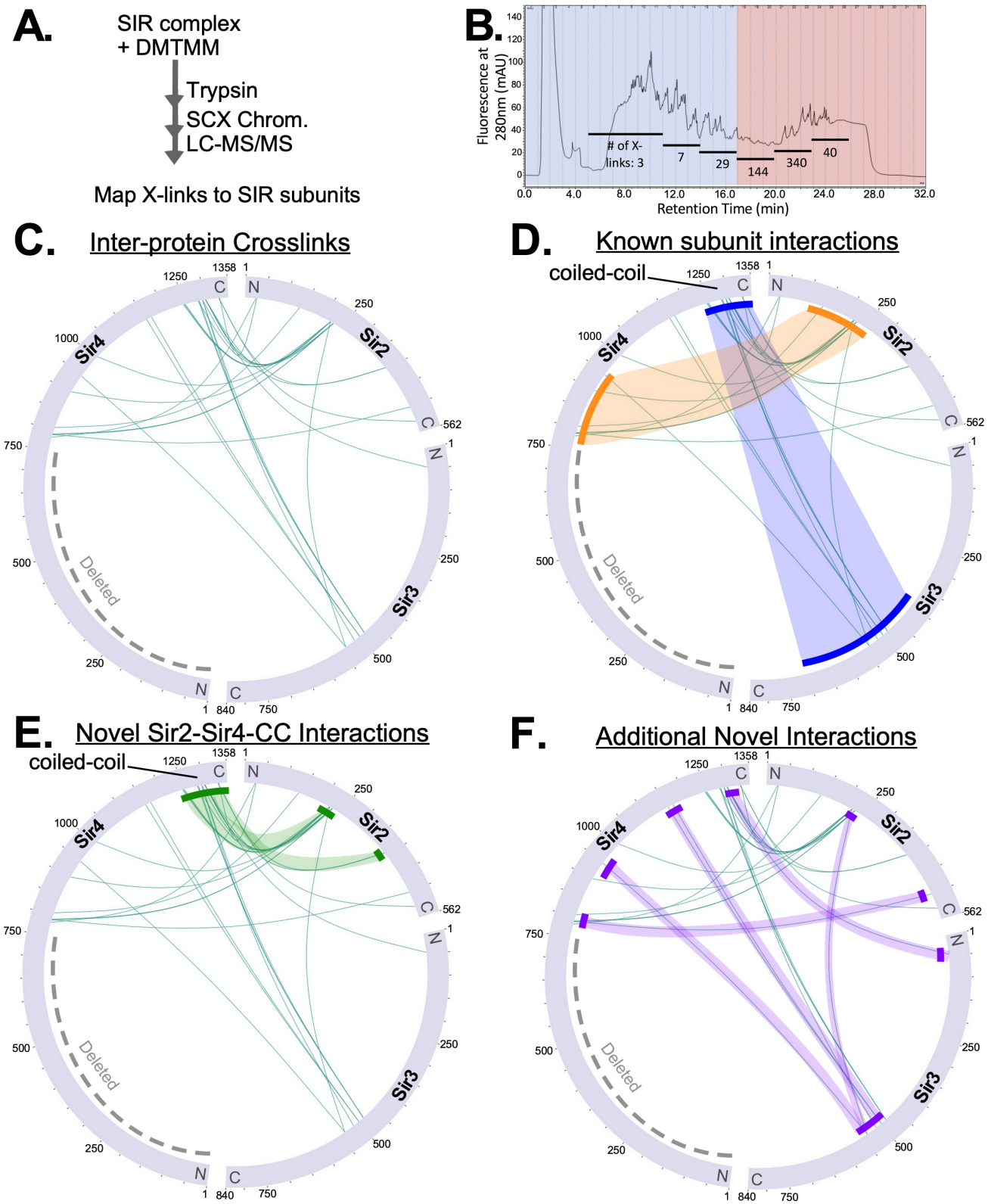

Figure 2. Crosslinking-mass spectrometry (XL-MS) identifies novel interactions between Sir2 and the coiled-coil of Sir4. A) Schematic for chemical crosslinking of the purified SIR complex using DMTMM, strong cation exchange (SCX), and tandem mass spectrometry (LC-MS/MS). B)

398 Chromatogram of peptides eluted from the SCX column. The elution was split into six fractions which
399 were individually analyzed by LC-MS/MS. Number of peptide crosslinks identified in each pool are
400 indicated. C) Wheel diagram of all inter-protein crosslinks identified in the XL-MS analysis of the
401 heterotrimeric SIR complex. Sir4-ΔN and Sir3Δwh were used. D-F) The same wheel diagram as in C)
402 with specific interactions highlighted: D) previously identified inter-subunit binding interfaces; E) novel
403 interactions between Sir2 and Sir4; F) additional novel interactions identified, including a triangulation of
404 position between Sir2, Sir3, and Sir4.
405
406

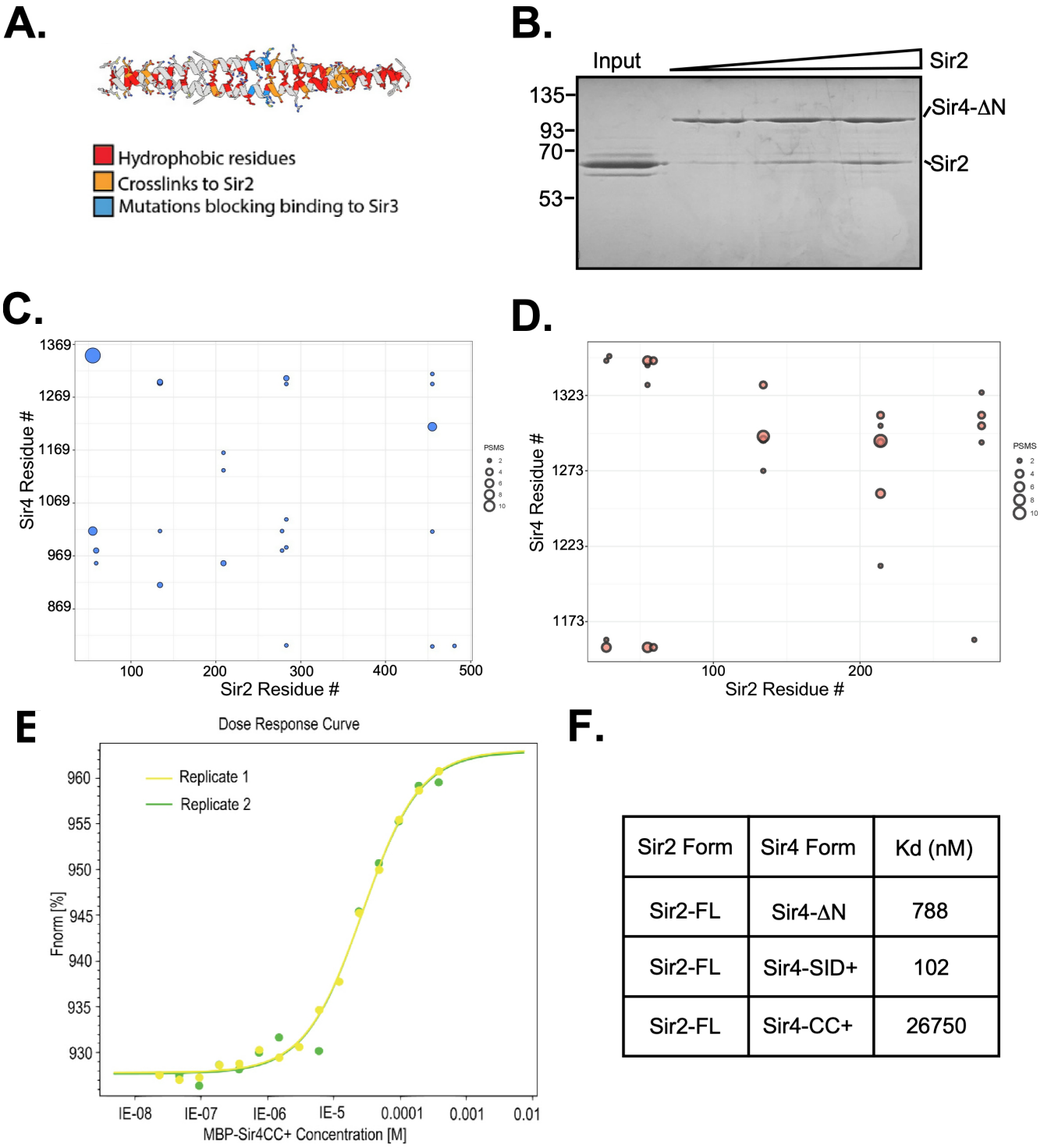

Sir2 Form	Sir4 Form	Kd (nM)
Sir2-FL	Sir4-ΔN	788
Sir2-FL	Sir4-SID+	102
Sir2-FL	Sir4-CC+	26750

Figure 3. Sir2 interacts with the coiled coil of Sir4. A) Ribbon diagram of the dimer of Sir4 coiled-coil domain. Highlighted residues include those that were identified as Sir2-interacting by cross-linking mass spectrometry (orange) and those that, when mutated, disrupt Sir3 interaction (blue). B) Purified full-length Sir2 was incubated with MBP-tagged Sir4-ΔN and the complex was isolated by amylose resin and resolved by SDS-PAGE and Coomassie stained. C) Matrix diagram depicting results from XL-MS of full-

413 length Sir2 and Sir4-ΔN, in the absence of Sir3. Sir2 axis is truncated due to no crosslinks occurring
414 beyond the displayed sequence. Datapoint circle size is indicative of the number of peptide-spectrum
415 matches (PSMs) at the given cross-link site. D) Matrix diagram depicting results from XL-MS of full-length
416 Sir2 and Sir4-CC+. Sir2 sequence is truncated due to no crosslinks occurring beyond the displayed
417 sequence. See methods for additional thresholding steps used for C) and D) analysis. E) Replicate
418 binding curves from microscale thermophoresis (MST) experiments with fixed concentration of labeled
419 Sir2 and MBP-Sir4CC+ titration range. F) Relative Kd measurements from MST experiments using the
420 given constructs.
421
422

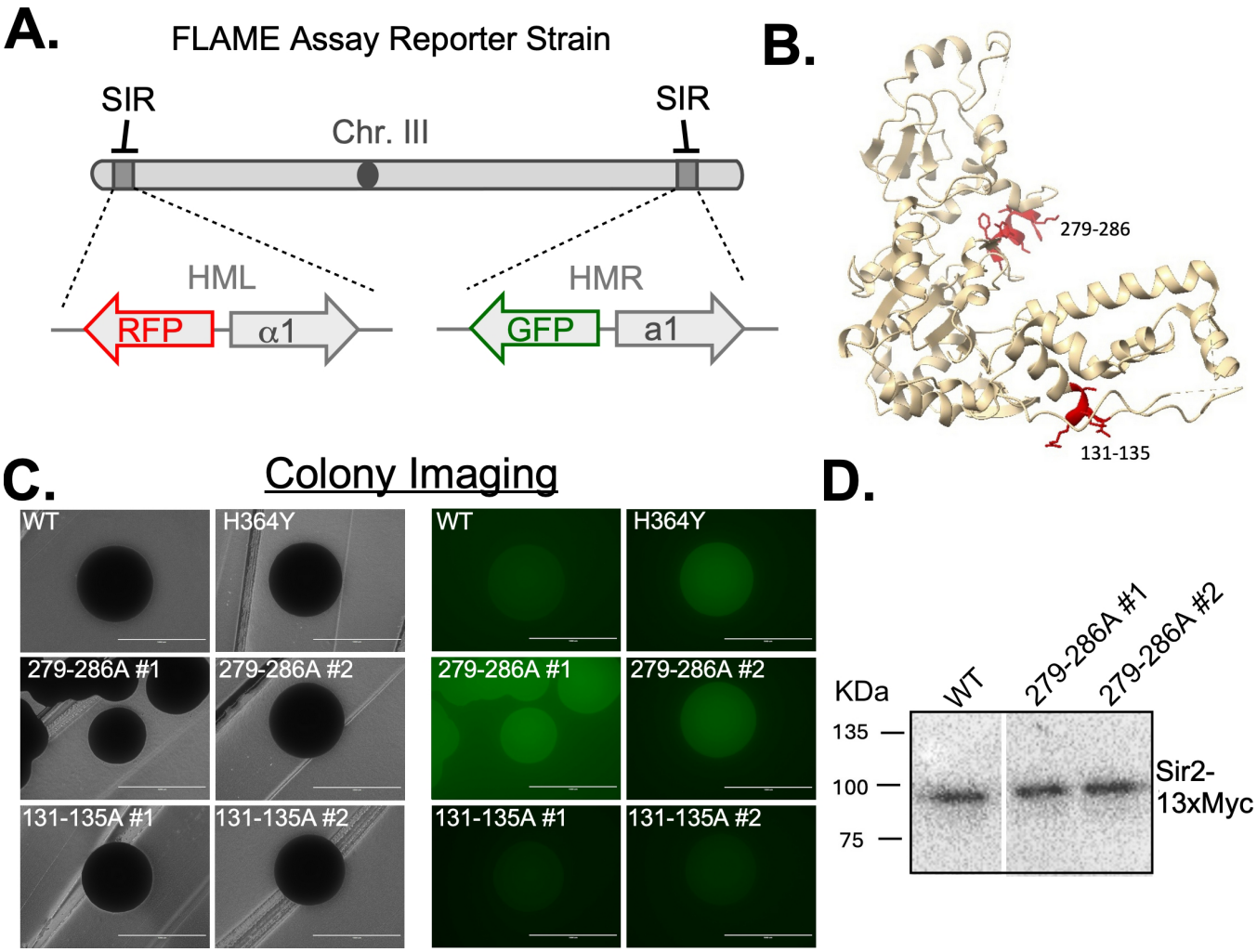

Figure 4. Identification of a novel regulatory region of Sir2. A) Schematic describing the FLAME assay system, previously developed [23, 24]. RFP and GFP are each substituted B) Ribbon diagram representation of Sir2 (PDB 4IAO) structure with two highlighted patches (red) that both make multiple crosslinks to the Sir4 coiled coil. C) Image of yeast colonies on the transillumination and GFP channels using the FLAME system strain. WT and Sir2 catalytic mutant (H364Y) are used as reference to image multiple isolates of strains mutated to alanine via CRISPR/Cas9 at Sir2131-135 and Sir2 279-286. One millimeter scale bar shown. D) Western analysis of myc-tagged Sir2 strains comparing wild-type and two Sir2 279-286A mutant isolates.

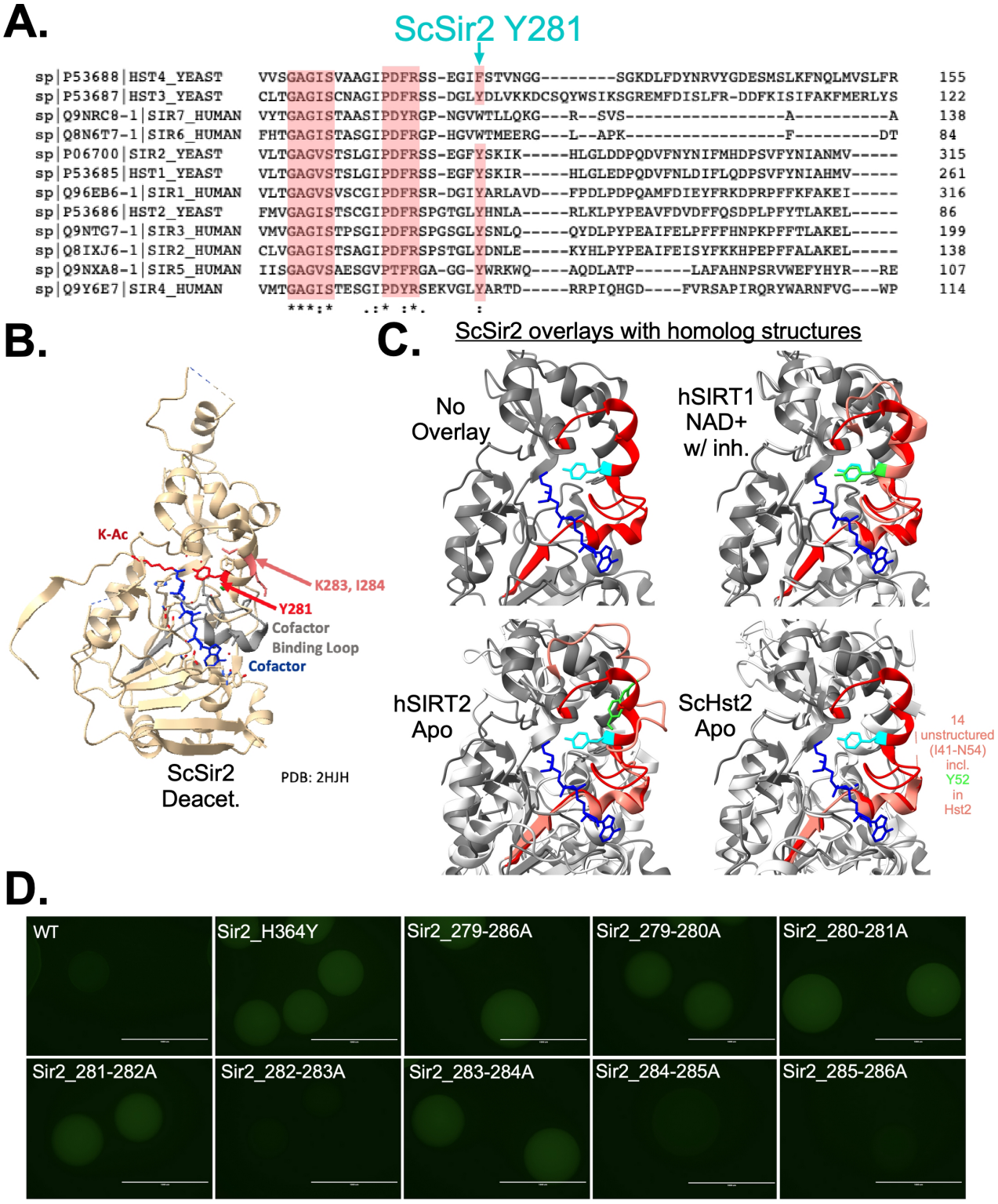

Figure 5. Conservation and analysis of key residues in the Sir2 cofactor binding loop extension. A) Alignment of all yeast and human sirtuins, highlighting the conservation in the cofactor binding loop extension and in the tyrosine residue at position 281 in budding yeast Sir2. B) Structure of budding yeast Sir2 (ScSir2) in the act of deacetylation with cofactor intermediate (blue) covalently attached to the lysine

440 being deacetylated (K-Ac). Key residues important for ScSir2 silencing (Y281, K283, I284) highlighted in
441 red. Unpublished PDB deposition 2HJH. C) Overlay of the 2HJH structure and structures of other sirtuins
442 in the apo and nucleotide bound forms, demonstrating the dynamics of the cofactor binding loop (dark
443 red for 2HJH, light red for other sirtuin) and the tyrosine sensor (ScSir2 Y281 in cyan, other sirtuin tyrosine
444 in green). Structures with a variety of cofactor binding status were used. The cofactor binding loop
445 extension of ScHst2 (*lower right*) is too flexible and is not resolved in the structure. PDB references: 4i5i
446 Chain A (hSIRT1), 1j8f Chain A (hSIRT2), 1q14 Chain A (ScHst2). D) Combinations of double mutants
447 within Sir2 279-286 were assessed by FLAME GFP assay. One millimeter scale bar shown.
448
449

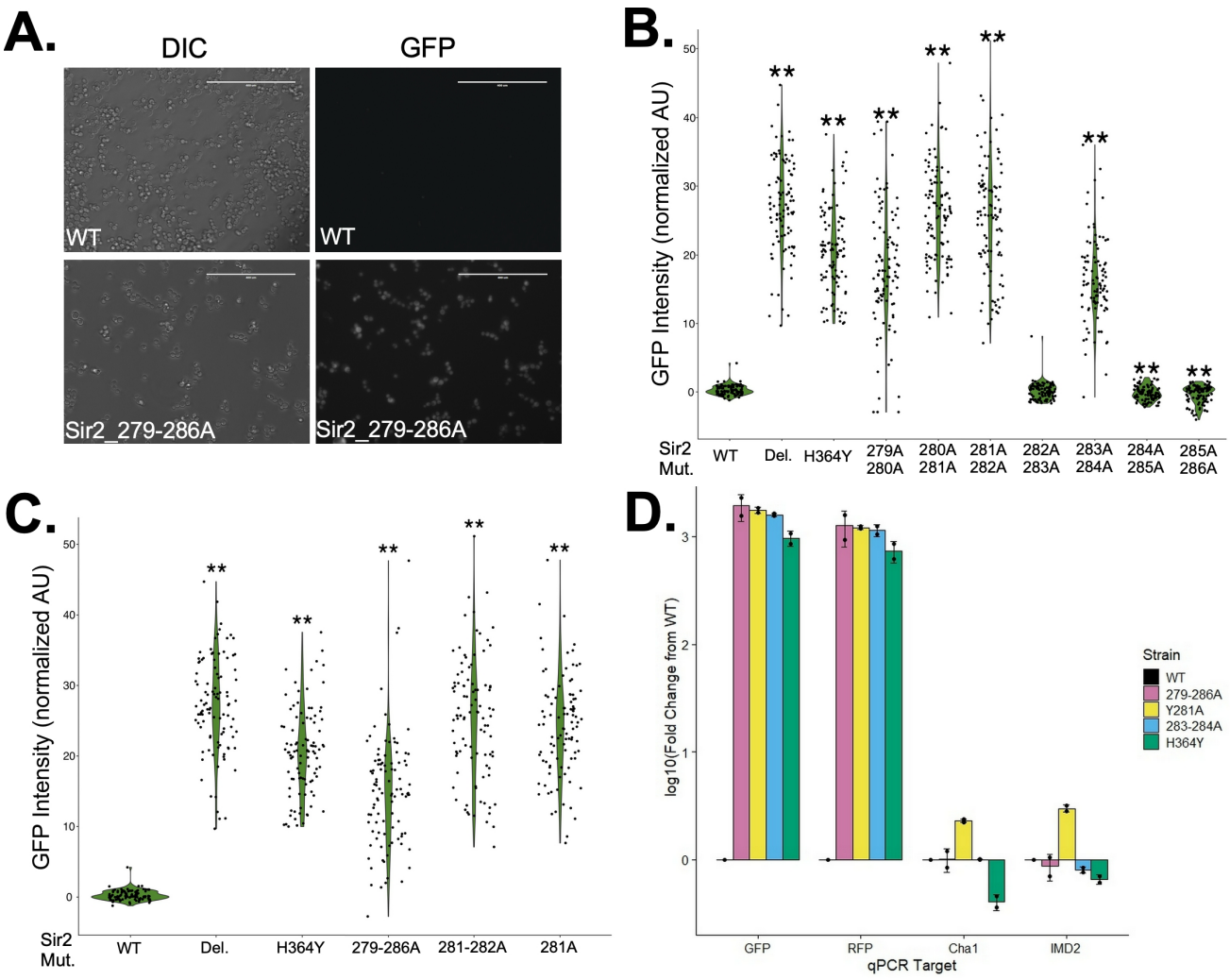

Figure 6. Sir2 Y281 alone and K283/I284 together are critical for SIR-dependent gene repression. A) Example of microscopy images, contrast and GFP channel, depicting WT and Sir2_279-286A FLAME strains. B) Single-cell quantification of GFP intensity for double mutants in the 279-286 patch of Sir2. C) Analysis of Sir2 Y281. ** over plots indicate t-test against WT yielded a p-value below 0.01. D) RT-qPCR determination of mRNA changes for SIR-regulated loci in indicated Sir2 mutants, log10 fold-change over WT from biological replicate strains. GFP and RFP genes located within HMR and HML, respectively.

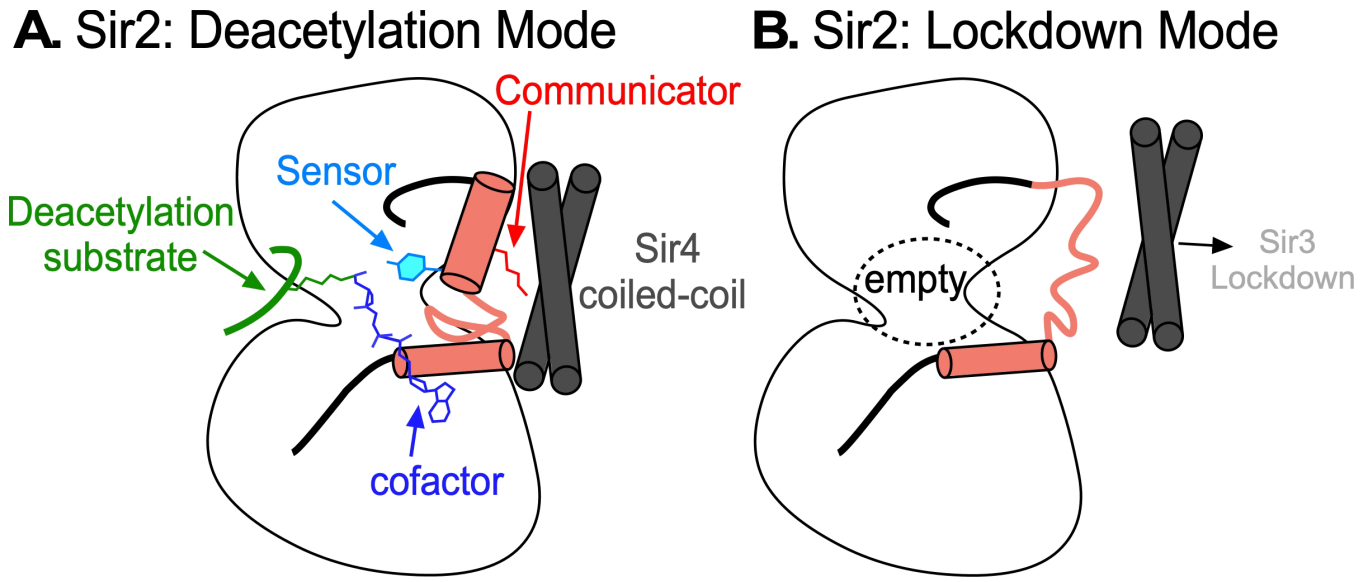

Figure 7. Proposed model for Sir2 conformational changes driving the two modes of the SIRc mechanism via communication with the Sir4 coiled-coil. A) In Deacetylation Mode, Sir2 is engaged with an acetylated histone substrate, using the NAD+ cofactor (blue) to drive removal of acetyl marks on histone lysine residues. In this state, the sensor, ScSir2 Y281 (cyan), detects the activity in the catalytic site, which promotes ordering of the helix that Y281 is on, the cofactor binding loop extension (light red), and orients the communicator residue(s), Sir2 K283 (red), which directly contacts the Sir4 coiled-coil to promote this mode of action. B) Once deacetylation is compete, the Sir2 catalytic site is empty, disengaging the sensor, which then leads to a disordered CBL extension, communicating to Sir4 that Sir3 can lockdown onto chromatin.

Acknowledgements

This work was funded by the NSF (Research Grant 2002231 from MCB to A.M.J and Graduate Research Fellowship 25A9567 to E.J.M.), the NIH (R35GM144358 to A.M.J.), and NCI Cancer Center Support Grant P30CA046934 to the University of Colorado Cancer Center. We would like to acknowledge Jacki Williams, Cassie Smith, Ari Rivera, Nahili Mohammed, Kim Miranda, and Aaron Issaian for technical assistance, Jasper Rine and his lab and John Wyrick and his lab for generous gifts of strains.

Conflict of Interest

The authors declare that they have no conflicts of interests with the contents of this article.

Author Contributions

J.K., E.J.M. and A.M.J. designed the research project; J.K., E.J.M., M.N., N.S., L.S., J.S., and N.H generated reagents; J.K., E.J.M., M.N., N.S., and L.S. performed experiments and analyzed preliminary data. J.K., E.J.M., K. H., and A.M.J. synthesized the data and wrote the manuscript.

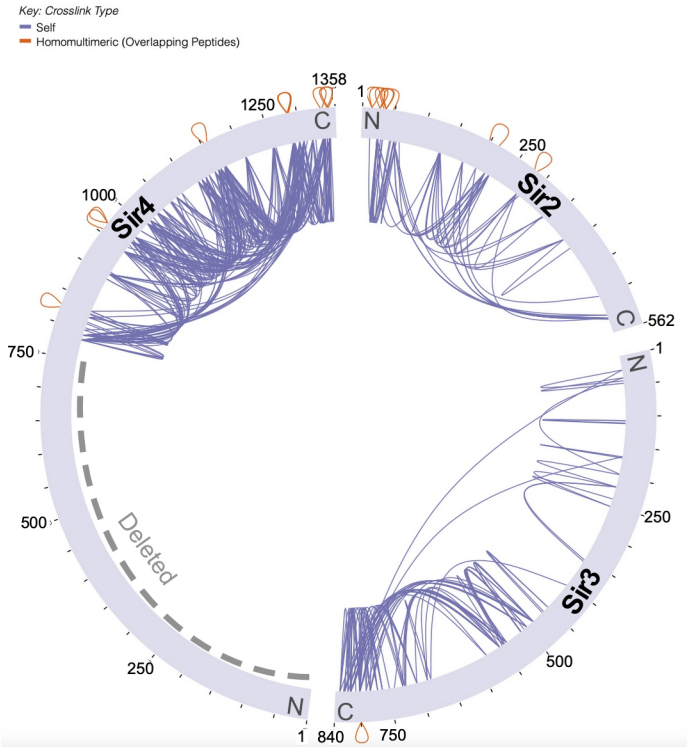

Supplemental Figure S1. Self crosslinks within the SIR complex. A) Example SIR complex assembly with Sir4ΔN, Sir3, and Sir2 incubation and elution with maltose. B) xiView schematic depicting the crosslinks within each Sir protein construct, including crosslinks with different parts of the protein (Self, purple) and two crosslinks between identical peptides (Homomultimeric, orange).

A.

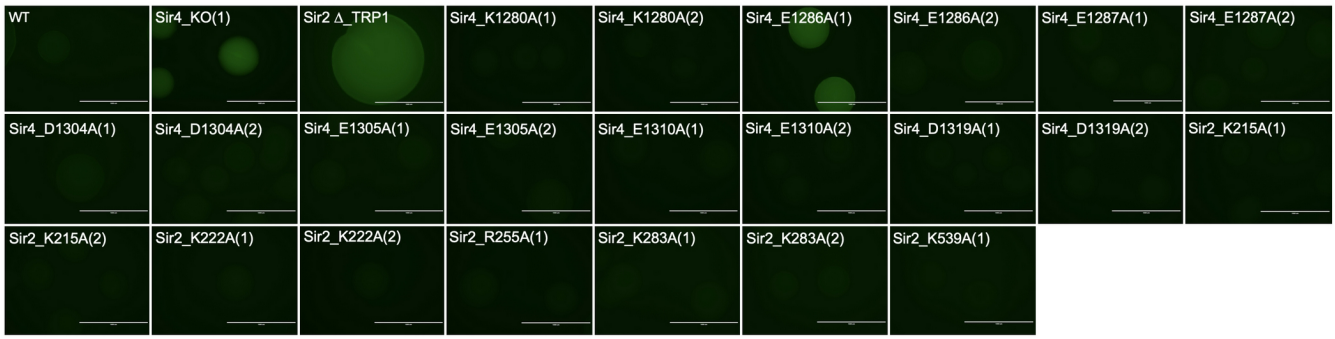

B.

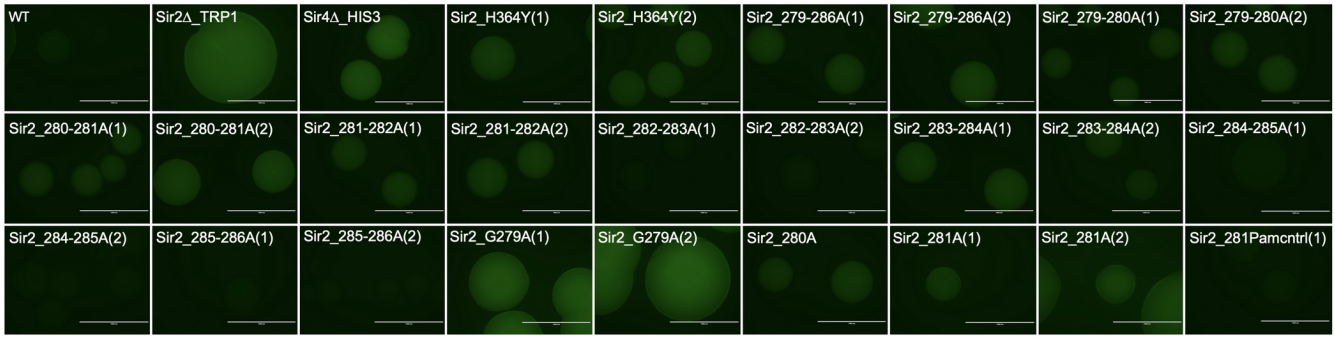

Supplemental Figure S2. Additional Colony FLAME Assay Results. A) GFP channel images from FLAME strains with alanine mutations of crosslink sites in Sir2 and Sir4. B) GFP channel images of FLAME strains of Sir2 mutations, including multiple isolates and a control for silent mutations of the Sir2 279-286 regions that includes the PAM site mutation used for all strains in the figure panel.

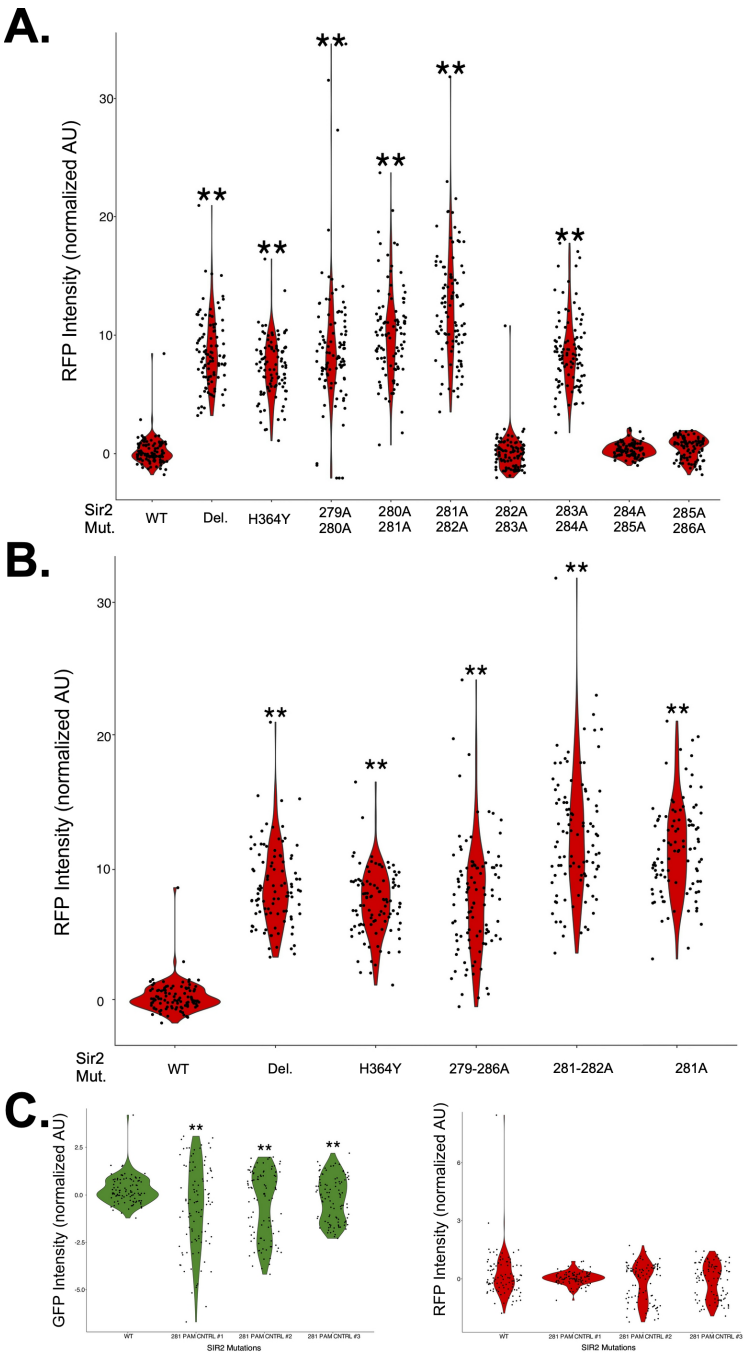

Supplemental Figure S3. Additional Single-Cell FLAME Assay results. A,B) RFP channel single cell FLAME results for indicated Sir2 mutants. C) GFP and RFP channel results for three strains with CRISPR-engineered PAM mutation only at the site used for mutation of Y281.

510

511 **Supplemental Table S1.** Crosslinked amino acids identified in experiments with Sir2 and constructs of

512 Sir4, identified with high-stringency filter.

513

514 **Supplemental Table S2.** Yeast strains used in this study.

515

516 **Supplemental Table S3.** RT-qPCR primers used in this study.

517

518 References

519

520 1. Rusche, L.N., Kirchmaier, A.L., and Rine, J. (2003). The establishment, inheritance, and function
521 of silenced chromatin in Saccharomyces cerevisiae. Annu Rev Biochem *72*, 481-516.
522 2. Kueng, S., Oppikofer, M., and Gasser, S.M. (2013). SIR proteins and the assembly of silent
523 chromatin in budding yeast. Annu Rev Genet *47*, 275-306.
524 3. Kaeberlein, M., McVey, M., and Guarente, L. (1999). The SIR2/3/4 complex and SIR2 alone
525 promote longevity in Saccharomyces cerevisiae by two different mechanisms. Genes Dev *13*,
526 2570-2580.
527 4. Vaziri, H., Dessain, S.K., Ng Eaton, E., Imai, S.I., Frye, R.A., Pandita, T.K., Guarente, L., and
528 Weinberg, R.A. (2001). hSIR2(SIRT1) functions as an NAD-dependent p53 deacetylase. Cell *107*,
529 149-159.
530 5. Johnson, A., Li, G., Sikorski, T.W., Buratowski, S., Woodcock, C.L., and Moazed, D. (2009).
531 Reconstitution of heterochromatin-dependent transcriptional gene silencing. Mol Cell *35*, 769-781.
532 6. Armache, K.J., Garlick, J.D., Canzio, D., Narlikar, G.J., and Kingston, R.E. (2011). Structural
533 basis of silencing: Sir3 BAH domain in complex with a nucleosome at 3.0 A resolution. Science
534 *334*, 977-982.
535 7. Wang, F., Li, G., Altaf, M., Lu, C., Currie, M.A., Johnson, A., and Moazed, D. (2013).
536 Heterochromatin protein Sir3 induces contacts between the amino terminus of histone H4 and
537 nucleosomal DNA. Proc Natl Acad Sci U S A *110*, 8495-8500.
538 8. Arnaudo, N., Fernandez, I.S., McLaughlin, S.H., Peak-Chew, S.Y., Rhodes, D., and Martino, F.
539 (2013). The N-terminal acetylation of Sir3 stabilizes its binding to the nucleosome core particle.
540 Nat Struct Mol Biol *20*, 1119-1121.
541 9. Yang, D., Fang, Q., Wang, M., Ren, R., Wang, H., He, M., Sun, Y., Yang, N., and Xu, R.M. (2013).
542 Nalpha-acetylated Sir3 stabilizes the conformation of a nucleosome-binding loop in the BAH
543 domain. Nat Struct Mol Biol *20*, 1116-1118.
544 10. Hsu, H.C., Wang, C.L., Wang, M., Yang, N., Chen, Z., Sternglanz, R., and Xu, R.M. (2013).
545 Structural basis for allosteric stimulation of Sir2 activity by Sir4 binding. Genes Dev *27*, 64-73.
546 11. Ehrentraut, S., Hassler, M., Oppikofer, M., Kueng, S., Weber, J.M., Mueller, J.W., Gasser, S.M.,
547 Ladurner, A.G., and Ehrenhofer-Murray, A.E. (2011). Structural basis for the role of the Sir3 AAA+
548 domain in silencing: interaction with Sir4 and unmethylated histone H3K79. Genes Dev *25*, 1835-
549 1846.
550 12. Chang, J.F., Hall, B.E., Tanny, J.C., Moazed, D., Filman, D., and Ellenberger, T. (2003). Structure
551 of the coiled-coil dimerization motif of Sir4 and its interaction with Sir3. Structure *11*, 637-649.
552 13. Oppikofer, M., Kueng, S., Keusch, J.J., Hassler, M., Ladurner, A.G., Gut, H., and Gasser, S.M.
553 (2013). Dimerization of Sir3 via its C-terminal winged helix domain is essential for yeast
554 heterochromatin formation. EMBO J *32*, 437-449.

555 14. Deshpande, I., Keusch, J.J., Challa, K., Iesmantavicius, V., Gasser, S.M., and Gut, H. (2019).
556 The Sir4 H-BRCT domain interacts with phospho-proteins to sequester and repress yeast
557 heterochromatin. EMBO J, e101744.
558 15. Leitner, A., Joachimiak, L.A., Unverdorben, P., Walzthoeni, T., Frydman, J., Forster, F., and
559 Aebersold, R. (2014). Chemical cross-linking/mass spectrometry targeting acidic residues in
560 proteins and protein complexes. Proc Natl Acad Sci U S A *111*, 9455-9460.
561 16. Beisel, C., and Paro, R. (2011). Silencing chromatin: comparing modes and mechanisms. Nat
562 Rev Genet *12*, 123-135.
563 17. Xu, F., Zhang, Q., Zhang, K., Xie, W., and Grunstein, M. (2007). Sir2 deacetylates histone H3
564 lysine 56 to regulate telomeric heterochromatin structure in yeast. Mol Cell *27*, 890-900.
565 18. Kueng, S., Tsai-Pflugfelder, M., Oppikofer, M., Ferreira, H.C., Roberts, E., Tsai, C., Roloff, T.C.,
566 Sack, R., and Gasser, S.M. (2012). Regulating repression: roles for the sir4 N-terminus in linker
567 DNA protection and stabilization of epigenetic states. PLoS Genet *8*, e1002727.
568 19. Martino, F., Kueng, S., Robinson, P., Tsai-Pflugfelder, M., van Leeuwen, F., Ziegler, M.,
569 Cubizolles, F., Cockell, M.M., Rhodes, D., and Gasser, S.M. (2009). Reconstitution of yeast silent
570 chromatin: multiple contact sites and O-AADPR binding load SIR complexes onto nucleosomes
571 in vitro. Mol Cell *33*, 323-334.
572 20. Oppikofer, M., Kueng, S., Martino, F., Soeroes, S., Hancock, S.M., Chin, J.W., Fischle, W., and
573 Gasser, S.M. (2011). A dual role of H4K16 acetylation in the establishment of yeast silent
574 chromatin. EMBO J *30*, 2610-2621.
575 21. Yang, B., Wu, Y.J., Zhu, M., Fan, S.B., Lin, J., Zhang, K., Li, S., Chi, H., Li, Y.X., Chen, H.F., et
576 al. (2012). Identification of cross-linked peptides from complex samples. Nat Methods *9*, 904-906.
577 22. Chen, Z.L., Meng, J.M., Cao, Y., Yin, J.L., Fang, R.Q., Fan, S.B., Liu, C., Zeng, W.F., Ding, Y.H.,
578 Tan, D., et al. (2019). A high-speed search engine pLink 2 with systematic evaluation for
579 proteome-scale identification of cross-linked peptides. Nat Commun *10*, 3404.
580 23. Farris, D., Saxton, D.S., and Rine, J. (2021). A novel allele of SIR2 reveals a heritable
581 intermediate state of gene silencing. Genetics *218*.
582 24. Saxton, D.S., and Rine, J. (2019). Epigenetic memory independent of symmetric histone
583 inheritance. Elife *8*.
584 25. Tanny, J.C., Dowd, G.J., Huang, J., Hilz, H., and Moazed, D. (1999). An enzymatic activity in the
585 yeast Sir2 protein that is essential for gene silencing. Cell *99*, 735-745.
586 26. Yuan, H., and Marmorstein, R. (2012). Structural basis for sirtuin activity and inhibition. J Biol
587 Chem *287*, 42428-42435.
588 27. Sanders, B.D., Jackson, B., and Marmorstein, R. (2010). Structural basis for sirtuin function: what
589 we know and what we don't. Biochim Biophys Acta *1804*, 1604-1616.
590 28. Ellahi, A., Thurtle, D.M., and Rine, J. (2015). The Chromatin and Transcriptional Landscape of
591 Native Saccharomyces cerevisiae Telomeres and Subtelomeric Domains. Genetics *200*, 505-521.
592 29. Armstrong, C.M., Kaeberlein, M., Imai, S.I., and Guarente, L. (2002). Mutations in
593 Saccharomyces cerevisiae gene SIR2 can have differential effects on in vivo silencing
594 phenotypes and in vitro histone deacetylation activity. Mol Biol Cell *13*, 1427-1438.
595 30. Wang, C.L., Landry, J., and Sternglanz, R. (2008). A yeast sir2 mutant temperature sensitive for
596 silencing. Genetics *180*, 1955-1962.
597 31. Garcia, S.N., and Pillus, L. (2002). A unique class of conditional sir2 mutants displays distinct
598 silencing defects in Saccharomyces cerevisiae. Genetics *162*, 721-736.
599 32. Sherman, J.M., Stone, E.M., Freeman-Cook, L.L., Brachmann, C.B., Boeke, J.D., and Pillus, L.
600 (1999). The conserved core of a human SIR2 homologue functions in yeast silencing. Mol Biol
601 Cell *10*, 3045-3059.
602 33. Mead, J., McCord, R., Youngster, L., Sharma, M., Gartenberg, M.R., and Vershon, A.K. (2007).
603 Swapping the gene-specific and regional silencing specificities of the Hst1 and Sir2 histone
604 deacetylases. Mol Cell Biol *27*, 2466-2475.
605 34. Chou, C.C., Li, Y.C., and Gartenberg, M.R. (2008). Bypassing Sir2 and O-acetyl-ADP-ribose in
606 transcriptional silencing. Mol Cell *31*, 650-659.

607 35. Rudner, A.D., Hall, B.E., Ellenberger, T., and Moazed, D. (2005). A nonhistone protein-protein
608 interaction required for assembly of the SIR complex and silent chromatin. Mol Cell Biol *25*, 4514-
609 4528.
610 36. Laughery, M.F., Hunter, T., Brown, A., Hoopes, J., Ostbye, T., Shumaker, T., and Wyrick, J.J.
611 (2015). New vectors for simple and streamlined CRISPR-Cas9 genome editing in Saccharomyces
612 cerevisiae. Yeast *32*, 711-720.
613